

Observation of temporal quantum interference via two collision-assisted two-step excitations

Xihua Yang,^{1,2,*} Zhenrong Sun,² and Zugeng Wang²

¹Department of Physics, Shanghai University, Shanghai 200444, People's Republic of China

²Department of Physics, East China Normal University, Shanghai 200062, People's Republic of China

(Received 17 March 2007; revised manuscript received 15 May 2007; published 16 October 2007)

We report the experimental observation of temporal quantum interference between two time-delayed 3S-3P-5S (or 4D) transition pathways created through two collision-assisted two-step excitation processes by using a single nanosecond laser pulse in the Na₂-Na system. It is clearly shown that the collisions offer a promising alternative to realize quantum interference in the time domain at room or higher temperatures despite the dephasing nature.

DOI: 10.1103/PhysRevA.76.043417

PACS number(s): 32.80.Qk, 34.10.+x, 42.50.Md

Just as classical optical interferences involve interferences in the space and time domains, there exist two kinds of quantum optical interferences. One refers to the interference between two or more different transition pathways connecting the same initial or final state in the frequency domain (e.g., spontaneous emission cancellation [1], coherent population trapping [2], etc.), and the other refers to the interference between two or more time-separated transition pathways connecting the same initial and final states in the time domain (e.g., temporal coherent control [3–5]). Laser-assisted collisions [divided into collisionally aided radiative excitation (CARE) and light-induced collisional energy transfer (LICET) [6]] provide an effective way for populating a particular atomic or molecular excited state, as collisions can supply or take away the extra energy to compensate for the energy defect between the photon and transition frequency. The collisions are generally thought to be dephasing in nature and detrimental to quantum coherence. However, the quantum coherence and interferences created through the laser-assisted collisions have been extensively studied. The CARE-induced quantum coherence and interference was first considered in pressure-induced extra resonance by Bloembergen [7] in four-wave mixing and by Grynberg [8] in nonlinear spectroscopy. Based on Grynberg's analysis, we have recently experimentally and theoretically studied the collision-induced quantum interferences in the frequency domain [9]. The LICET-induced quantum coherence and interference has been theoretically analyzed by Berman [10] and experimentally observed by Debarre [11] and Cahuzac [12]. Moreover, the temporal quantum interference has also been experimentally demonstrated in radiatively assisted collisions between Rydberg atoms [13]. In the previous experiments of temporal quantum interference, the two time-delayed transition pathways were produced either by using an atomic or a molecular supersonic beam to pass through two spatially separated cw laser beams [3,4], or by using two time-delayed laser pulses [5]. In this paper, we report the experimental observation of temporal quantum interference between two time-delayed 3S-3P-5S (or 4D) transition pathways realized through the special two collision-assisted two-step excitation processes by using a single laser pulse in the Na₂-Na system.

Figure 1 schematically shows the relevant energy levels in the Na₂-Na system together with the excitation processes driven by a single ns laser pulse and the stimulated emission 5S (or 4D)-4P. As analyzed in Refs. [14–16], there exist two collision-assisted two-step excitation processes for populating the 5S (or 4D) state when the laser wavelength is tuned near the resonant transition 3P-5S (or 4D). The first one is the atomic collision-assisted two-step excitation (process I), i.e., the off-resonant collision-assisted excitation of the sodium atom from the 3S state to the 3P_{1/2,3/2} states [the mean time interval between the laser-assisted Na-Na (and Ar) collisions is τ_1], and the subsequent resonant or nearly resonant excitation 3P_{1/2,3/2}-5S (or 4D) (indicated with the two thin lines). The second one is the molecule-atom hybrid excitation (process II), that is, the excitation of sodium molecules from the X¹ Σ_g^+ state to the A¹ Σ_u^+ state followed by the Na₂-Na collision energy transfer [$\text{Na}_2(\text{A}^1\Sigma_u^+) + \text{Na}(3\text{S}) \rightarrow \text{Na}^*(3\text{P}_{1/2,3/2}) + \text{Na}_2(\text{X}^1\Sigma_g^+)$] to excite the sodium atom from the 3S state to the 3P_{1/2,3/2} states (the mean time interval between the Na₂-Na collisions is τ_2), and the subsequent resonant or nearly resonant excitation 3P_{1/2,3/2}-5S (or 4D) (indicated with the two thick lines). Ob-

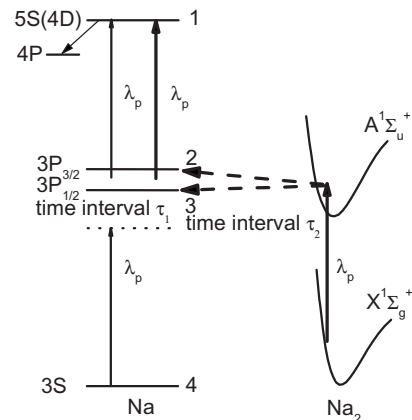


FIG. 1. The relevant energy levels in the Na₂-Na system and the two collision-assisted two-step excitation processes. The two time-delayed 3S-3P-5S (or 4D) transition pathways are created through the atomic collision-assisted two-step excitation (indicated with the two thin lines) and molecule-atom hybrid excitation (indicated with the two thick lines) by the same single ns laser pulse when the laser wavelength λ_p is tuned near the resonant transition 3P-5S (or 4D).

*Corresponding author: yangxih@yahoo.com.cn

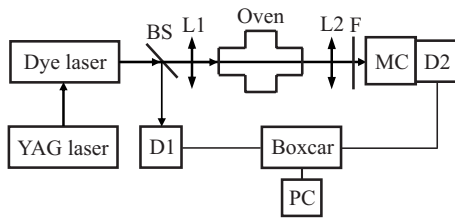


FIG. 2. The experimental setup. BS, beam splitter; L1 and L2, lens; F, infrared filter; MC, monochromator; D1, triggering detector; and D2, infrared detector.

viously, two time-delayed 3S-3P-5S (or 4D) transition pathways are created through the two collision-assisted two-step excitation processes I and II, where the time delay corresponds to the difference of the two mean time intervals τ_2 and τ_1 . The two indistinguishable 3S-3P-5S (or 4D) transition pathways driven by the same single laser pulse are coherent and would interfere with each other, so Ramsey fringes [17] could be observed in the population of the 5S (or 4D) state by tuning the laser frequency near the resonant transition 3P-5S (or 4D) under certain experimental conditions. As discussed by Krökel [15], the 5S (or 4D) state population resulting from other processes, such as two-photon absorption and energy pooling collisions, are at least two orders of magnitude less than that from the above two excitation processes I and II, and therefore can be neglected.

The experimental setup is shown in Fig. 2. The tunable laser used throughout the experiments is a dye laser pumped by a Q-switched Nd:YAG laser. The pulse duration and line-width of the dye laser are about 15 ns and 0.1 cm^{-1} , respectively. The laser wavelength is tuned in the measured range of 614.5–617.0 or 567.7–570.0 nm, which lies in the absorption band of the $X^1\Sigma_g^+-A^1\Sigma_u^+$ transition in sodium dimer. The laser beam with 2 mm in diameter is focused by a lens with a focal length of 70 cm to the center of a cross heat-pipe oven with a heating length of 22 cm and containing about 20 g pure sodium. The oven temperature is typically kept at about 760 K, corresponding to the sodium atomic and molecular densities of about 3.8×10^{16} and $1.4 \times 10^{15} \text{ cm}^{-3}$, respectively [18]. The forward directional radiation with about an 8 mrad divergence angle, which is approximately the same as that of the pumping laser beam, is introduced into a monochromator after passing through an infrared bandpass filter to eliminate the residual pump beam. The forward infrared stimulated emission is detected by a PbSe detector for the radiation 5S-4P at about $3.41 \mu\text{m}$ (or a PbS detector for the radiation 4D-4P at about $2.34 \mu\text{m}$). The signals are recorded by a PC after integration by a boxcar.

The solid line in Fig. 3(a) shows the measured excitation spectrum for generating the stimulated radiation 5S-4P with the sample temperature of about 760 K, pulse energy of about 2.0 mJ, and Ar buffer gas pressure of about 0.18 bar. It can be seen that an envelope corresponding to the two collision-broadened resonant absorption $3P_{1/2}$ -5S and $3P_{3/2}$ -5S is modulated by Ramsey fringes. The two highest peaks stand at the two atomic resonant absorption wavelengths of 615.43 and 616.08 nm, where the frequency separation between them is about 17.20 cm^{-1} , corresponding to the energy separation of the 3P doublet. The frequency separation

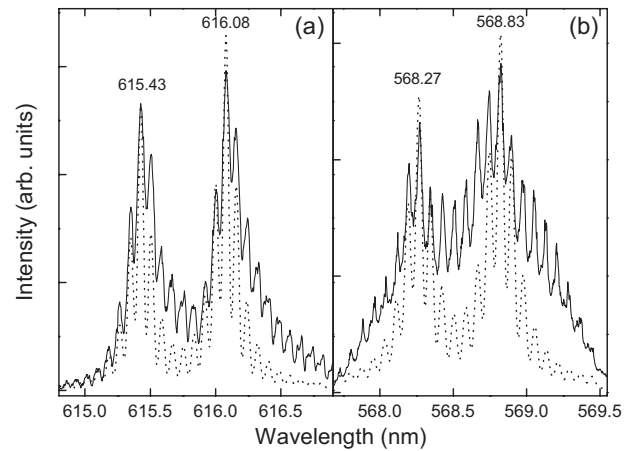


FIG. 3. Experimental (solid lines) and calculated (dotted lines) excitation spectra for generating the stimulated emission 5S-4P (a) and 4D-4P (b) with the sample temperature of about 760 K, pulse energy of about 2.0 mJ, and Ar buffer gas pressures of about 0.18 bar (a) and 0.30 bar (b), respectively.

between two neighboring interference fringes is about 2.15 cm^{-1} ; it means that the time difference of the two collision-assisted excitation processes I and II is about 15.5 ps. In addition, we also measure the excitation spectrum in the backward direction and find the fringes still exist, which indicates that the fringes should not come from some nonlinear optical wave-mixing processes.

In order to confirm that the fringes do come from interference between two time-delayed collision-assisted two-step transition pathways, we further measure the excitation spectrum for generating the stimulated radiation 4D-4P to test whether the fringes can also appear under certain conditions. As shown in Fig. 3(b) with the solid line, Ramsey fringes superimposed on an envelop corresponding to the two collision-broadened resonant absorption $3P_{1/2,3/2}$ -4D are observed as well under almost the same conditions as those of the preceding experiment except for the Ar buffer gas pressure of about 0.30 bar. The two highest peaks are also centered at the two resonant absorption wavelengths of 568.27 and 568.83 nm. The frequency separation (about 2.46 cm^{-1}) between two neighboring fringes corresponds to the time difference (about 13.6 ps) of the two excitation processes I and II. It can be seen from the different frequency separation between two neighboring fringes in Figs. 3(a) and 3(b) that the fringes in Fig. 3 are not the consequence of some experimental artifacts, such as the interference on the cell windows, as the fringes from the interference on the cell windows should have equal frequency separation between two neighboring fringes in Figs. 3(a) and 3(b).

It may seem strange that the collisions can induce coherence, as it is generally thought that the collisions destroy coherence. However, as theoretically analyzed by Berman [10] and experimentally demonstrated by Debarre [11] and Cahuzac [12], quantum coherence and interference can be produced through the LICET process in spite of its basically inelastic character. According to the analyses in Refs. [6,12], we perform a theoretical calculation by solving the time-dependent Schrödinger equation of the probability amplitude

of the 5S (or 4D) state. As to the time evolution of the two collision-assisted two-step excitation processes I and II for populating the 5S (or 4D) state, as shown in Fig. 1, if we assume that the onset of the interaction of the laser pulse with the quantum system is at arbitrary time $t=t_0$, then the sodium atom in the 3S state is driven into a virtual state (about 700 cm^{-1} away from the 3P state and shown with the dotted line) by one-photon absorption at time $t=t_0$, and the sodium molecule in the $X^1\Sigma_g^+$ state is excited to the $A^1\Sigma_u^+$ state by one-photon absorption at time $t=t_0$ as well; the subsequent evolutions of the two kinds of collisions would also begin at the same time $t=t_0$. As is well-known, the mean time interval between two collisions is equal to the inverse of the collisional decay rate (its definition is similar to that of the lifetime of an atomic or a molecular excited state), which can be treated as definite under a certain experimental condition. Thus at time $t=t_0+\tau_1$, i.e., after the mean time interval τ_1 between the laser-assisted Na-Na (and Ar) collisions, the sodium atom is excited to the 3P state from the virtual state through the laser-assisted Na-Na (and Ar) collisions and subsequently excited to the 5S (or 4D) state by further absorbing a photon; at time $t=t_0+\tau_2$, i.e., after the mean time interval τ_2 between the Na_2^* -Na collisions, the sodium atom can also be excited to the 3P state through the Na_2^* -Na collision-energy-transfer and subsequently excited to the 5S (or 4D) state by further absorbing another photon. Consequently, two time-delayed 5S (or 4D) state probability amplitudes with a definite time delay corresponding to the difference $\delta\tau=\tau_2-\tau_1$ are realized through the two collision-assisted two-step excitation processes I and II. Correspondingly, at any definite time after the onset of the interaction of the laser pulse with the quantum system, the two first-step excitations in the processes I and II would begin simultaneously at this definite time and the following two kinds of collisions would also start to evolve at the same definite time; subsequently, there always exist two time-delayed 5S (or 4D) state probability amplitudes with a definite time delay $\delta\tau$ through the two excitation processes I and II. Therefore, with the time evolution of the interaction of the laser pulse with the quantum system, a series of two time-delayed 5S (or 4D) state probability amplitudes with a definite time delay $\delta\tau$ are formed, which would interfere with each other, and Ramsey fringes could be observed in the 5S (or 4D) state population under certain conditions.

Following the experimental excitation processes, we consider an atomic system consisting of four states: 1, 2, 3, and 4, corresponding to the states 5S (or 4D), $3P_{3/2}$, $3P_{1/2}$, and 3S, respectively. We denote the detuning of the laser field with frequency ω_L from the 3P-5S (or 4D) transition with frequency ω as $\Delta=\omega_L-\omega$, the Rabi frequency of the laser field with amplitude E coupling the 3P and 5S (or 4D) states as $\Omega=\mu E/\hbar$ [μ is the dipole moment for the transition 3P-5S (or 4D)], and the decay rate of the 5S (or 4D) state as γ_1 , which depends not only on the 5S (or 4D) state natural lifetime, but also on the collisions. The dynamic evolution of the 5S (or 4D) state probability amplitude $C_1(t)$ can be written as

$$\frac{d}{dt}C_1(t) = -i\Omega e^{i\Delta t}C_2(t) - \gamma_1 C_1(t), \quad (1)$$

where $C_2(t)$ is the probability amplitude of the 3P state, which has two contributions; the first is the laser-assisted

collision excitation 3S-3P with a mean time interval of τ_1 , and the second is the Na_2^* -Na collision-energy-transfer induced excitation 3S-3P with a mean time interval of τ_2 . The order of τ_1 and τ_2 is about 10^2 ps [19,20], and the durations of the two type collisions (about 1 ps) are much smaller than τ_1 and τ_2 [21]. As analyzed in Refs. [6,12], the two probability amplitudes for populating the 3P state through the excitation processes I and II can be readily calculated with the perturbation theory under the assumption of a Van der Waals collisional interaction. When the laser field is tuned near the 3P-5S (or 4D) transition, since the laser tuning range (about 70 cm^{-1}) is far smaller than both the $X^1\Sigma_g^+-A^1\Sigma_u^+$ transition bandwidth and the detuning [about -720 cm^{-1} (or 630 cm^{-1})] of the laser from the resonant transition 3S-3P, the two 3P state probability amplitudes can be regarded as independent of the laser frequency ω_L and denoted as β_1 and β_2 , respectively; it indicates that the line profile in Fig. 3(a) [or Fig. 3(b)] corresponds indeed to the collision-broadened resonant absorption 3P-5S (or 4D). We assume that the decay rate of the 3P state is γ_2 ; then the probability amplitude $C_2(t)$ can be written as $C_2(t)=\beta_1 e^{-\gamma_2 t} + \beta_2 e^{-\gamma_2(t-\delta\tau)}$. Consequently, the probability amplitude $C_1(t)$ also has two components [denoted as $C_1(t)=b_1(t)+b_2(t)$]. If the onset time of the interaction of the pulse with the quantum system is arbitrarily set at time $t_0=-\tau_1$, then at time $t=0$, one probability amplitude for populating the 5S (or 4D) state is realized through process I and the probability amplitude $b_1(t)$ is $b_1(t) = \frac{-i\Omega\beta_1 e^{-\gamma_1 t} [e^{i(\Delta-\gamma_2+\gamma_1)t}-1]}{i\Delta-\gamma_2+\gamma_1}$; and at time $t=\tau_2-\tau_1=\delta\tau$, the other probability amplitude for populating the 5S (or 4D) state is realized through process II, and the probability amplitude $b_2(t)$ is $b_2(t) = \frac{-i\Omega\beta_2 e^{i\Delta\delta\tau-\gamma_1(t-\delta\tau)} [e^{i(\Delta-\gamma_2+\gamma_1)(t-\delta\tau)}-1]}{i\Delta-\gamma_2+\gamma_1}$. Therefore the total probability for populating the 5S (or 4D) state [taking into account the 3P doublet ($k=2$ and 3)] after the laser pulse is equal to the modulus squared of the sum of the integrations of the probability amplitudes $b_1(t)$ and $b_2(t)$ over time, which can be expressed as

$$|C_1(\infty)|^2 \propto \sum_{k=2}^3 \frac{\Omega_k^2}{|i\Delta_k - \gamma_{2k} + \gamma_1|^2} [1 + \beta^2 e^{2\gamma_1 \delta\tau} + 2\beta e^{\gamma_1 \delta\tau} \cos \Delta_k \delta\tau], \quad (2)$$

where β is the ratio β_2/β_1 , $\Delta_k=\omega_L-\omega_{1k}$ is the detuning of the laser from the transition k to 1 with frequency ω_{1k} , $\Omega_k = \mu_{1k} E/\hbar$ is the Rabi frequency of the laser field coupling the states 1 and k , and γ_{2k} is the decay rate of the state k . It can be seen from Eq. (2) that the first two terms in the square bracket correspond to the two independent 3S-3P-5S (or 4D) transitions for populating the 5S (or 4D) state, whereas the last term corresponds to the interference between them. Whether the interference is constructive or destructive depends on the term $\cos \Delta_k \delta\tau$ being positive or negative. Therefore by tuning the laser frequency near the transition 3P-5S (or 4D), the 5S (or 4D) state population would exhibit Ramsey fringes and the frequency separation between two neighboring fringes is equal to $1/\delta\tau$.

The dotted lines in Figs. 3(a) and 3(b) show the calculated results with the consideration of the line broadening from the

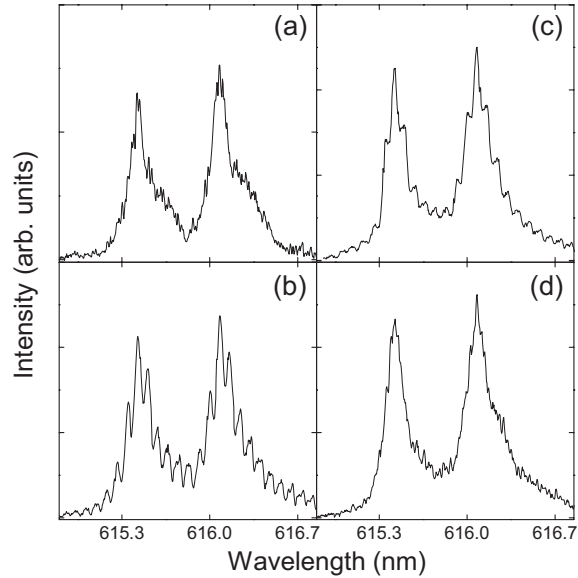


FIG. 4. Experimental excitation spectra for generating the stimulated emission 5S-4P with the pulse energy of about 2.0 mJ, Ar buffer gas pressure of about 0.18 bar, and sample temperatures of about 750 K (a), 760 K (b), 765 K (c), and 770 K (d), respectively.

resolution of the monochromator. According to the data in Refs. [19,20], the decay rates are set as follows: $\gamma_1 = 3.1 \text{ cm}^{-1}$, $\gamma_{22} = 0.7 \text{ cm}^{-1}$, and $\gamma_{23} = 0.9 \text{ cm}^{-1}$ in Fig. 3(a), and $\gamma_1 = 4.2 \text{ cm}^{-1}$, $\gamma_{22} = 1.0 \text{ cm}^{-1}$, and $\gamma_{23} = 1.2 \text{ cm}^{-1}$ in Fig. 3(b), respectively. The two mean time intervals τ_2 and τ_1 are on the order of 10^2 ps and the difference between them is on the order of 10 ps [19–21], so the time delay $\delta\tau$ is set according to the experimental data to be 15.5 and 13.6 ps in Figs. 3(a) and 3(b), respectively. The factor $\beta e^{\gamma_1 \delta\tau}$ is set to equal 1 in both Figs. 3(a) and 3(b), as the most obvious fringes are observed under the conditions. It can be seen that the calculated results are in reasonable agreement with the experimental ones. The discrepancy in the red detuning sides of the peaks is due to the experimental fact [22] that the decay rates in the red detuning sides are larger than that in the blue ones, which is not included in the calculation. Note that, as discussed in Refs. [15,19], the above values of the ratio β and decay rates γ_1 and γ_2 are only approximate ones, and the reliable data about them at a particular sample temperature and buffer gas pressure do not exist so far (these parameters only affect the contrast of the fringes or linewidth of the resonance profile). However, the main physical picture and the most distinct feature of temporal quantum interference, i.e., the envelop corresponding to the two collision-broadened resonant absorption $3P_{1/2,3/2}$ -5S (or 4D) modulated by Ramsey fringes, are clearly presented in both our experimental and calculated results.

Since the quantum interference is realized through the two collision-assisted two-step excitation processes, where the collision plays an essential role, the fringes should be very

sensitive to the sample temperature or buffer gas pressure. Figure 4 shows the sample temperature dependences of the excitation spectra for generating the stimulated radiation 5S-4P. Obviously, a very sensitive dependence of the fringes on the sample temperature is displayed. As shown in Figs. 4(b) and 4(c), although no distinct increase of the frequency separation between two neighboring interference fringes can be observed due to the small increase of the temperature (about 5 K), an obvious decrease of the contrast of the interference fringes is seen. Moreover, the temperature variation of about 10 K would wash out the fringes, as shown in Figs. 4(a) and 4(d). The extremely sensitive dependence of the fringes on the experimental temperature is due to the fact that the contrast of the interference fringes $[2\beta e^{\gamma_1 \delta\tau} / (1 + \beta^2 e^{2\gamma_1 \delta\tau})]$ is determined by the ratio β , time delay $\delta\tau$, and decay rate γ_1 , all of which critically depend on the collisions. The distinct fringes can only be observed when it should be simultaneously satisfied that the product $\beta e^{\gamma_1 \delta\tau}$ nearly equals one, and the time delay $\delta\tau$ could not be longer than the 5S (or 4D) state radiative time or the characteristic time of any collision-induced dephasing process. The simultaneous satisfaction of these conditions indicates that only under a suitable sample temperature and buffer gas pressure can the interference fringes be clearly observed. In addition, the various collision-induced dephasing processes, such as the escape of the atoms and molecules out of the laser beam, collision-ionization, and collision-quenching, would also destroy the quantum interference. These may be the main reasons that a small decrease or increase of the temperature would lead to the disappearance of the fringes. The extreme sensitivity of the interference fringes to the buffer gas pressure in the 3S-3P-5S excitation is observed as well. This can account for Krökel's [15] and our [16] previous failures to observe the fringes. It should be noted that, as seen in Figs. 4(a)–4(d), since the molecular concentration increases with the increase of the sample temperature, the disappearance of the fringes enables us to exclude that the fringes result from any molecular transitions.

In conclusion, we have experimentally observed the temporal quantum interference between the two time-delayed 3S-3P-5S (or 4D) transition pathways created through the special two collision-assisted two-step excitation processes by using a single ns laser pulse in the Na₂-Na system. Our present and previous [9] results further support the argument [7,8,10–12] about collision-induced quantum coherence and interference, and clearly indicate that the collisions offer a promising alternative to realize quantum interference in both the time and frequency domains at room or higher temperatures in spite of the dephasing nature.

X. Yang wishes to thank S. Y. Zhu at HKBU for theoretical analysis and discussion of the manuscript. This research was supported by Shanghai Postdoctoral Foundation (Grant No. 05R214118), Shanghai Education Committee Foundation (Grant No. 06AZ094), and Shanghai Leading Academic Discipline Project (Grant No. T0104).

- [1] S. Y. Zhu and M. O. Scully, *Phys. Rev. Lett.* **76**, 388 (1996); H. R. Xia, C. Y. Ye, and S. Y. Zhu, *ibid.* **77**, 1032 (1996).
- [2] G. Alzetta *et al.*, *Nuovo Cimento Soc. Ital. Fis., B* **36**, 5 (1976); E. Arimondo, *Prog. Opt.* **35**, 257 (1996).
- [3] Y. V. Baklanov, B. Y. Dubetsky, and V. P. Chebotayev, *Appl. Phys.* **9**, 171 (1976); A. Huber, B. Gross, M. Weitz, and T. W. Hansch, *Phys. Rev. A* **58**, R2631 (1998).
- [4] R. N. Zare, *Science* **279**, 1875 (1998); S. Chu, *Nature (London)* **416**, 206 (2002).
- [5] M. M. Salour, *Rev. Mod. Phys.* **50**, 667 (1978); V. Engel and H. Metiu, *J. Chem. Phys.* **100**, 5448 (1994); V. Blanchet, C. Nicole, M. A. Bouchene, and B. Girard, *Phys. Rev. Lett.* **78**, 2716 (1997).
- [6] A. Bambini and P. R. Berman, *Phys. Rev. A* **35**, 3753 (1987); P. R. Berman, F. Schuller, and G. Nienhuis, *ibid.* **42**, 459 (1990).
- [7] N. Bloembergen, *Laser Spectroscopy IV* (Springer, Berlin, 1979), p. 340; Y. Prior, A. R. Bogdan, M. Dagenais, and N. Bloembergen, *Phys. Rev. Lett.* **46**, 111 (1981).
- [8] G. Grynberg and P. R. Berman, *Phys. Rev. A* **41**, 2677 (1990).
- [9] X. H. Yang *et al.*, *Chin. Phys. Lett.* **19**, 334 (2002); X. H. Yang and H. K. Xie, *Phys. Rev. A* **67**, 063807 (2003); X. H. Yang *et al.*, *J. Phys. B* **38**, 2519 (2005).
- [10] P. R. Berman, *Phys. Rev. A* **22**, 1838 (1980); **22**, 1848 (1980); P. R. Berman and A. Bambini, *ibid.* **50**, 623 (1994).
- [11] A. Debarre, *J. Phys. B* **15**, 1693 (1982).
- [12] P. Cahuzac and P. E. Toschek, *Phys. Rev. Lett.* **40**, 1087 (1978).
- [13] M. J. Renn and T. F. Gallagher, *Phys. Rev. Lett.* **67**, 2287 (1991).
- [14] W. Muller and I. V. Hertel, *Opt. Commun.* **45**, 400 (1983).
- [15] D. Krökel *et al.*, *Appl. Phys. B: Photophys. Laser Chem.* **37**, 137 (1985).
- [16] Z. G. Wang and H. R. Xia, *Molecular and Laser Spectroscopy* (Springer, Berlin, 1991), p. 174.
- [17] N. F. Ramsey, *Rev. Mod. Phys.* **62**, 541 (1990).
- [18] A. N. Nesmeyanov, *Vapor Pressure of the Chemical Elements* (Academic, New York, 1963), p. 423.
- [19] E. L. Lewis, *Phys. Rep.* **58**, 47 (1980); N. Allard and J. Kielkopf, *Rev. Mod. Phys.* **54**, 1103 (1982).
- [20] E. K. Kraulinya, E. K. Kopeikina, and M. L. Janson, *Chem. Phys. Lett.* **39**, 565 (1976); J. Huennekens and A. Gallagher, *Phys. Rev. A* **27**, 1851 (1983).
- [21] S. Lemont *et al.*, *J. Chem. Phys.* **66**, 4509 (1977); T. Sizer II and M. G. Raymer, *Phys. Rev. Lett.* **56**, 123 (1986); *Phys. Rev. A* **36**, 2643 (1987).
- [22] J. L. Carlsten, A. Szoke, and M. G. Raymer, *Phys. Rev. A* **15**, 1029 (1977).